









Beyond the Veil of Similarity: Quantifying Semantic Continuity in Explainable AI

Qi Huang¹, Emanuele Mezzi², Osman Mutlu³, Miltiadis Kofinas⁴, Vidya Prasad⁵, Shadnan Azwad Khan⁶, Elena Rangelova⁷, and Niki van Stein¹

¹ *Leiden University*, Leiden, The Netherlands

{q.huang,n.van.stein}@liacs.leidenuniv.nl

² *Vrije Universiteit Amsterdam*, Amsterdam, The Netherlands

³ *Wageningen Food Safety Research*, Wageningen, The Netherlands

⁴ *University of Amsterdam*, Amsterdam, The Netherlands

⁵ *Eindhoven University of Technology*, Eindhoven, The Netherlands

⁶ *Sorbonne University*, Paris, France

⁷ *Netherlands eScience center*, Amsterdam, The Netherlands

Abstract. We introduce a novel metric for measuring semantic continuity in Explainable AI methods and machine learning models. We posit that for models to be truly interpretable and trustworthy, similar inputs should yield similar explanations, reflecting a consistent semantic understanding. By leveraging XAI techniques, we assess semantic continuity in the task of image recognition. We conduct experiments to observe how incremental changes in input affect the explanations provided by different XAI methods. Through this approach, we aim to evaluate the models' capability to generalize and abstract semantic concepts accurately and to evaluate different XAI methods in correctly capturing the model behaviour. This paper contributes to the broader discourse on AI interpretability by proposing a quantitative measure for semantic continuity for XAI methods, offering insights into the models' and explainers' internal reasoning processes, and promoting more reliable and transparent AI systems.

Keywords: Semantic Continuity · Explainable AI · Machine Learning Interpretability · Semantic Analysis

1 Introduction

Human intelligence can project objects and events to higher-order semantics. Starting from concrete objects it then generates abstractions that are invariant to the change of the environments in which those objects were initially identified. Over the years, given the growing power of representation shown by deep learning (DL) models, specifically deep neural networks (DNNs), researchers have started to wonder whether this capacity to abstract is only exclusive to humans or also embedded in the neural architecture. The field of Explainable AI (XAI) aims to find the answer to this question, highlighting the features contributing to

a specific prediction realized by a neural network (or other machine learning model).

Over time, one of the concepts that characterized XAI called *continuity* has emerged and was highlighted in [18]. It can be framed as the capacity of the XAI method, i.e., the explainer, to behave consistently with the model behaviour. More concretely, the explanations of similar model inputs that result in similar model outputs (confidence) should also correspondingly give similar explanations.

In this work, we investigate *semantic continuity*, which we outline as “similar semantics should have similar explanations”. We first define the scope of this work and a general background in XAI in Section 2. We then list related literature and the motivation of our proposed solution in Section 3. We then define the term semantic continuity in Section 4 and propose a new metric to measure the semantic continuity of a given model and explainer. In Section 5, we investigate the semantic continuity in the image domain, and we discuss the results in 6. Lastly, in Section 7 we summarize our findings and provide our final remarks.

2 Explainable AI

The field of XAI, motivated by the imperative to understand the inner workings of AI models, has undergone many advancements in recent years. This has resulted in various explanation methods being developed that may be broadly categorized into attribution-based, model-based, and example-based explanations [15]. Particularly, attribution-based methods provide insights into the importance of the features in a model by assigning importance values or ranks based on the relevance of these features to final predictions. There are global explanation methods such as Global Sensitivity Analysis [32], which attribute importance to features for a given model on a global level, and there exist various methods for single predictions (local methods), such as perturbation-based, gradient-based, surrogate-based, and propagation-based methods [27]. This discussion mainly focuses on perturbation-based and gradient-based methods for single predictions.

3 Related Work

Over the past years, several evaluation frameworks and metrics have emerged to assess the performance and compare different XAI methods with each other. One of these measures is continuity. Continuity is a critical aspect that ensures the stability and generalizability of XAI solutions and is often associated with robustness. In [2], an AutoXAI framework is proposed that automates the selection of XAI solutions where continuity is a property that plays a significant role. Understanding this property becomes even more crucial in scenarios such as Part-Prototype Image classifiers, where continuity directly influences user trust and the model’s ability to generalize [17].

To evaluate the continuity property in XAI solutions, several tools and methodologies have been developed, with some focusing on image-based tasks [12]. Toolkits designed for XAI evaluation in continuity tests on images include: Quantus [6], Safari [7], XAI-Bench [13], and BAM [35]. Additionally, more generic XAI toolkits like Captum [11] and OmniXAI [36] are available. However, the continuity metrics utilized in these tools require further verification.

Examining perturbed inputs has revealed complexities surrounding continuity, particularly when the perturbations lead to misinterpretations and inconsistencies in explanation outcomes. Two types of misinterpretations come to light: one where a perturbed input with different highlighted features receives the same prediction label, and another, where a perturbed input with similar highlighted features is assigned a different prediction label [7].

Additionally, the assumption that explanations and model outcomes are directly comparable has been brought into question. Such as in [5], where experimental demonstrations with image classification tasks, employing various perturbation techniques (Gaussian noise variation, spatial rotation, spatial translation, and latent sampling) are tested, utilizing distance measures such as Maximum Mean Discrepancy and Lipschitz Continuity. The findings support the notion that the outcome is affected by the perturbation techniques and the distance measures employed. It is concluded that the continuity test as it stands, can be easily biased towards desired results by employing a particular combination of perturbation technique and distance measure. This prompts the need for a more rigorous assessment of continuity.

The study in [3] investigates the effect of Adversarial Perturbations (APs), and subtle disruptions in input data on DNNs. It uses GradCAM to generate explainability maps and shows a decrease in correlation coefficients between Layered GradCAM outputs after a DeepFool attack. Correspondingly, the research in [34] is focused on the problem of semantic discontinuity of deep learning models, where small perturbations in the input space tend to cause semantic-level interference to the model output, which is explained by the flaws in choosing the training targets. The need to study continuous perturbations of the input data is also argued in [8], especially for model interpretability. The authors have addressed the causes for the previously observed fragility of many attribution XAI methods and propose enhanced metrics and improving robustness via adversarial training. The focus of those and similar papers is only on studying the DL method itself. While adversarial robustness is very important, in the context of explaining the model’s behaviour in semantic terms, the potential influence of an explainer has not been researched.

A system for visual analytics and understanding of CNNs, VATUN, is presented in [20]. Again, the focus is on studying the sensitivity to and preventing adversarial attacks and is also limited to GradCAM images. Similarly, Perturber, introduced in [30], is a web application offering interactive comparison of base and adversarially trained CNN models. Our proposed approach is generic for any data modality, DL model architecture, and attribution explainer. Also, both

VATUN and Perturber are interactive approaches and do not include a metric for quantifying (semantic) continuity, which we propose in this work.

As far as we know, here we are the first to define the notion of “semantic continuity” in the XAI context. In the inspirational publication [18], 12 properties of explainers have been defined for their objective and systematic evaluation. Continuity considers how continuous is the explanation function learned by the explainer. A continuous function ensures that small variations in the input lead to small changes in the explanation. Continuity also adds to generalizability beyond a particular input, which is specifically useful for domain experts who are not (X)AI experts. Having primarily their needs in mind, we have extended the notion of continuity to semantic continuity as a valuable property of an explainer.

4 Semantic Continuity

To define semantic continuity, we first look at the definition of continuity in the context of explainable AI from the work [18]. The definition of continuity in [18] is loosely defined as “similar inputs should have similar explanations”. We expand this idea with the notion of “semantic continuity” so that “*semantically* similar inputs should have similar explanations.” This definition brings us to the following hypothesis:

- A slight change in the input will correspond to a slight change in the output, which is the result of the explainer.
- Given the explanation of a reference prediction (the base case), the bigger the input change, the bigger the change between the explanation of the current output and the explanation of the initial (reference) output. This will yield an increasing monotonic correlation between changes in explanations and changes in the original input (images).

Definition 1. Let \mathbf{x}_0 denote the reference input data, and f be a function that applies a semantic variation θ with a domain Θ on the input data, resulting in $\mathbf{x}_i = f(\mathbf{x}_0; \theta_i)$. Let M be a deep learning model and $E(M)$ the explainer of the model. We define semantic continuity as follows:

$$\theta_j - \theta_0 > \theta_i - \theta_0 \Rightarrow D(E(M(\mathbf{x}_j)), E(M(\mathbf{x}_0))) > D(E(M(\mathbf{x}_i)), E(M(\mathbf{x}_0))), \quad (1)$$

$\forall \theta_i, \theta_j \in \Theta$, where θ_0 corresponds to an identity transformation, i.e. $\mathbf{x}_0 = f(\mathbf{x}_0; \theta_0)$ and $E(M(\mathbf{x}_0))$ corresponds to its explanation. The function D corresponds to a distance function between the two explanations.

To test whether XAI methods are semantically continuous, given that the predictor is a perfect predictor that is also semantically continuous, and thus respects the mathematical definition on which we ground the concept of semantic continuity, we propose the following approach: First, given a trained predictor (for example a DL model) for a boolean classification task, we define one or more semantic variations we can apply to the data. For example in the case of image classification, we can apply image transformation techniques such as

rotation, contrast change and cropping, which do not alter the semantic meaning of the image. On the other hand, we can also define a gradual transformation from one class to the other class (and therefore gradually changing semantics). Next, we apply the predictor to predict images generated using the semantic variations and subsequently apply an explainer to get the feature attribution map for the prediction. Finally, we can measure the distance between the original (non-transformed) image and the semantic variation of the input image and we can measure the distance between the two feature attribution maps given by the explainer. These distances should increase monotonically when applying larger semantic variations and the distances between inputs should be correlated to distances of the explanations derived by the explainer.

4.1 Proof-of-concept Experiment

To investigate the semantic continuity of XAI methods, the simplest case study consists of binary classification. We will first explore semantic continuity by considering the case in which the machine learning model must distinguish between triangles and circles, where the grayscale images contain only one uniform triangle or circle positioned in the centre of a uniform background. We selected this case study as proof of concept as the task is simple and can be easily manipulated. In addition, we can assume (and verify) that the model on this task is more or less a perfect predictor.

Considering that the case study is a binary classification task, we build a Convolutional Neural Network (CNN) of 2 hidden layers, which is sufficient for a model to learn the features that enable it to distinguish between triangles and circles (100% test accuracy).

Generation of Datasets with Semantic Variations Once the model has been trained, we generate datasets that enable us to measure the semantic continuity of XAI methods in different scenarios. As shown in Figure 1, we analyze three possible cases of semantic variation and continuity:

- Rotation: the explainer is semantically continuous concerning the rotation of triangles. To check this property, we generate a dataset of 100 images of the same triangle on the same background. The dataset is a sequence of images with the triangle rotating clockwise by one degree.
- Contrast: the explainer is semantically continuous concerning variations in the background contrast. To check this property, we built a dataset composed of 200 images. The first 100 are images of triangles, and the second 100 are circles. In this case, the progressive change consists of a constantly diminishing contrast of the shape with the background until the shape is no longer recognizable.
- Transition: the most complex semantic transformation. The rotation and contrast are fixed. The dataset, composed of 100 images, is a sequence where the starting image depicts a circle and the ending image - a triangle. The shape gradually changes from a circle to a triangle in the in-between images.

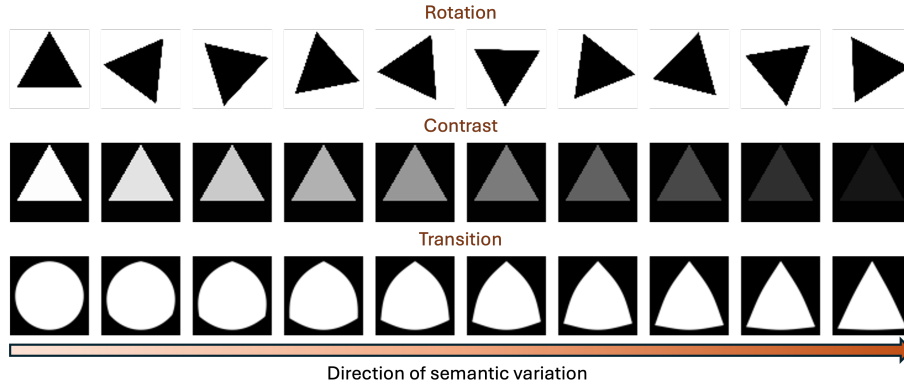


Fig. 1: Demonstrations of the data used for the proof-of-concept experiment.

Comparing Different XAI Methods The (pre)trained model is used in each of the three scenarios above to measure the semantic continuity of different explainers.

We test the semantic continuity of RISE [22], LIME [25], GradCAM [28], and SHAP [16] explainers, as these are popular and well-established XAI methods. In this proof-of-concept experiment, we assume that the model is a perfect predictor and the output of the model adheres to the semantic continuity definition.

Based on this assumption, it is possible to check whether it respects the mathematical assumption in Equation (1) through qualitative analysis and quantitative correlations between the changes in input and explainer output.

To understand the extent to which the XAI output under gradual semantic variations respects monotonicity, the verification is composed of two phases, the first consisting of visual inspection and the second consisting of the application of a correlation metric apt for monotonicity checking to investigate whether a positive change in the input is correlated with a positive change in the explainer output. The correlation metrics that we use to quantify semantic continuity are the Pearson [21], Spearman’s [31] and Kendall’s Tau [9] metric.

4.2 From *Perfect Predictor* to *Imperfect Predictor*

As the first proof-of-concept experiment relies on a perfect predictor, we refine our definition of semantic continuity to be able to verify semantic continuity of the XAI method not only when the model is a perfect predictor but also when the model output is not semantic continuous. In addition, the binary classification of geometric shapes is fairly straightforward for the classifier being evaluated, and we would like to show the applicability of our proposed approach in a more realistic real-world setting. It is noteworthy that in Definition 1, we aim to directly establish a connection between the semantic changes in input data and the changes in post hoc explanations generated by XAI methods. However, recall one of the fundamental requirements of XAI methods, correctness, which aims

to achieve high faithfulness of explanations w.r.t. the to-be-explained model [18]. Our implicit assumption for Definition 1, is the classifier can consistently perceive the semantic changes in **test time** such that it is feasible to evaluate the semantic continuity using XAI methods. In the next evaluation scenario, this assumption or constraint is lifted. Following a similar vein to the previous proof-of-concept Shape datasets, we consider the binary classification of human facial information, which is a much more challenging task for the machine learning model, and hence, the XAI explainers are exposed to a more noisy situation where the model is not always providing accurate predictions. The concept and the criterion of semantic continuity are now re-formulated.

Definition 2 (Semantic variation). *Let θ denote a semantic variation in the range $[\Theta_A, \Theta_B]$, $\Theta_A < \Theta_B$. We let f be a deterministic function that applies such variations θ on \mathbf{x}_0 , resulting in $\mathbf{x}_i = f(\mathbf{x}_0; \theta_i)$, where θ_i is a real number that quantifies the scale of such variations. Here, the function f and the variation indicator θ_i firstly satisfies:*

$$P(H(\mathbf{x}_i) = \Theta_A \mid x = \mathbf{x}_i) + P(H(\mathbf{x}_i) = \Theta_B \mid x = \mathbf{x}_i) = 1, \quad (2)$$

where $H(\cdot)$ is a fixed (hypothetically) perfect semantic percipient, and P is the probability symbol. Secondly, for any pairs of valid (θ_i, θ_j) , the following causal property shall be held:

$$\theta_j > \theta_i \Rightarrow P(H(\mathbf{x}_j) = \Theta_B \mid x = \mathbf{x}_j) > P(H(\mathbf{x}_i) = \Theta_B \mid x = \mathbf{x}_i). \quad (3)$$

Definition 2 establishes the concept for a data-dependent, unique, deterministic, and controlled semantic variation process between the two semantics (or domains or concepts). Based on this definition, we now provide formal definitions of semantic continuity for both predictors and XAI methods (explainers).

Let $M(x)$ be a machine learning model that determines the semantics for an input x , and a post-hoc explainer $E(M; x)$ of M . Notably, we only consider explainers that implicitly or explicitly produce a real-valued heatmap over the entire x or a feature importance score for each element in x .

Definition 3 (Predictor semantic continuity). *Given a reference data point \mathbf{x}_0 of semantic Θ_A and a variation function $f(\cdot; \theta)$ that can transform \mathbf{x}_0 from Θ_A to Θ_B as defined in Definition 2. We say the model M is semantically continuous between Θ_A and Θ_B shortly, $\xrightarrow{\Theta_{A,B}}$, on \mathbf{x}_0 if for any valid pair of (θ_i, θ_j) :*

$$\theta_j > \theta_i \Rightarrow P(M(x) = \Theta_B \mid x = \mathbf{x}_j) > P(M(x) = \Theta_B \mid x = \mathbf{x}_i), \quad (4)$$

where $\mathbf{x}_k = f(\mathbf{x}_0; \theta_k)$, a semantic variation following Definition 2, and $P(M(x) = \Theta_B \mid x = \mathbf{x}_k)$ denotes the probability (confidence) of \mathbf{x}_k to be an instance of domain Θ_B , estimated by model M .

Definition 4 (Explainer semantic continuity). *Similarly, given with a predictive model M , a semantic variation function $f(x; \theta)$ as defined in Definition 2,*

and a reference data point \mathbf{x}_0 , we say the explainer E is $\overrightarrow{\Theta_{A,B}}$ regarding M on \mathbf{x}_0 if for any valid pair of (θ_s, θ_t) :

$$P_B(M; \mathbf{x}_s) > P_B(M; \mathbf{x}_t) \Rightarrow D(E(M; \mathbf{x}_s), E(M; \mathbf{x}_0)) > D(E(M; \mathbf{x}_t), E(M; \mathbf{x}_0)), \quad (5)$$

where $\mathbf{x}_k = f(\mathbf{x}_0; \theta_k)$, $P_B(M; \mathbf{x}_k)$ is short for $P(M(x) = \Theta_B \mid x = \mathbf{x}_k)$, and $D(\cdot, \cdot)$ is a distance metric that quantifies the discrepancy between outputs of the explainer E .

Notably, when testing semantic continuity for explainers as defined in Definition 4, we don't assume any size relationship between the paired indicators of variations. Speaking in general, when we relate these new definitions to the previous one, Definition 1 relies on the assumption that the to-be-explained predictor holds Definition 3 almost surely, but will contradict the requirement of *correctness* for XAI methods when this assumption is not upheld.

4.3 Synthesis of the human facial dataset

With the aforementioned formal definitions of semantic continuity, we propose to design and create a binary classification (class A vs class B) dataset \mathcal{S} that satisfies Definition 2 but maximally prohibits a strong baseline model from being $\overrightarrow{\Theta_{A,B}}$ on all reference points in \mathcal{S} .

In this research, particularly, we consider classification on artificially generated human faces, where the two non-overlapping classes are **with glasses** and **without glasses**. The training data is generated using stable diffusion [26], and all unrealistic samples are manually removed. Figure 2 depicts several randomly chosen examples of our training data. The test dataset is constructed using In-



Fig. 2: Examples of training data used in our second experiment.

terFaceGAN [29] and SEGA [1]. Both are generative models that are capable of smoothly transforming a source image of one semantic to an image of another

non-overlapping target semantic while preserving other semantics of the source image during the transformation. The transformation process can be exclusively controlled by a real-valued indicator showing the degree of likeness to the target semantic. Once we determine a sequence of such variation indicators and a starting reference image, it is feasible to generate test data that follows our Definition 2, where the generative model itself serves as both the variation function f and the semantic percipient H . We give an example of a series of consistently generated test images in Figure 3, where from left to right, the generative model gradually adds a pair of glasses to the face of a girl.



Fig. 3: An example sub-series of a test case in our second experiment. The left-most image illustrates a randomly generated face of a non-real girl without glasses. From left to right, we use generative models to gradually add a pair of *half-rimless* glasses to the images.

Practically, since both generative models are not perfect (regarding humans), it is important to manually inspect their outcomes and discard all series of images that have an unreliable target image as displayed, e.g., in Figure 4. However, we preserve several of these data for analyzing the explainer continuity under the case where Definition 2 does not hold for human-level semantic percipient.



Fig. 4: An example sub-series of a test case that does not hold for Definition 2. The context here is the same as that of Figure 3. However, as the semantic variation (indicator) increases, the fidelity of images being **with glasses** does not increase in the end. And the final image, if talking from human inspections, is not fully convincing to be **with glasses**.

5 Experimental Setup

5.1 Shape Dataset

To explore the (easier to analyse) proof-of-concept scenario related to the capacity of the explainers to capture the semantic continuity in images, we prepare three gray-scale image datasets, each related to a different semantic scenario:

- Rotation: fixing the background contrast, this dataset contains 100 images of equilateral triangles with different degrees of rotation. Starting from a base triangle, we apply a progressive rotation to the shape, allowing it to complete a 120-degree rotation.
- Contrast: fixing the rotation, this dataset contains 100 images of triangles and 100 images of circles with different background contrast. Starting from the base case of a triangle and a circle with maximum gray-level contrast, we progressively diminish the contrast with the background resulting in a shape that is indistinguishable from the environment.
- Transition: fixing rotation and contrast, this dataset contains x images of shapes. Starting from a triangle, the images show a progressive transition until the final image is one of a circle.

The model used [14] to test the semantic continuity of XAI methods, tested with the above datasets, has been trained on the Simple geometric shapes dataset [19].

5.2 Synthesis facial dataset

In section 4.3, the methodology for creating the dataset has been introduced. In total, the training data contains 1000 balanced samples and the test set contains 100 balanced samples. Among the test samples, 48 samples with the label **no glasses** are chosen to be the reference image for semantic variations, where each of them is gradually shifted towards the **with glasses** class twenty times uniformly. This results in 1,008 images for testing the explainers’ semantic continuity.

Regarding the classifier, we choose the well-known baseline model ResNet [4] with 18 convolution layers and a Sigmoid output layer. The model is fitted exclusively on the training data from scratch using binary cross entropy loss and Adam optimizer [10] for about 20 epochs. As a result, the ResNet-18 achieves 100% predictive accuracy on the 100 test samples.

For consistency across the setups between experiments, following setups for the Shape dataset, we evaluated instance-wise semantic continuity of RISE, LIME, GradCAM, and KernelSHAP explainers. We choose mean squared deviation and Wasserstein distance as the distance metric (regarding D_I) for Definition 4) in quantitative analysis.

5.3 Software

For the experiments, the uniform implementation of the XAI explainers in the Deep Insight and Neural Network Analysis (DIANNA) [24], [23] python library has been used.

6 Results

The results section is organized into two subsections: i) results and insights from the proof-of-concept shape dataset to show the outcome of comparisons of different explainers and correlation metrics and ii) results of semantic continuity of explainers on the complex facial image classification task with realistic images.

6.1 Proof-of-concept Results: Shape Dataset

To calculate the extent to which changes in the input lead to changes in the output, we calculate the correlation between the independent variable x , which represents the change in the input, and the dependent variable y , which represents how explanations vary.

The distance metrics considered are the Pearson correlation, Spearman’s correlation and Kendall’s Tau correlation. Considering that the ideal result consists of a monotonic function, that would be able to show the increasing change that affects the output once the input is modified, these correlation metrics have been selected on the basis of their capacity to capture monotonicity.

For each transformation (contrast, rotation and gradual change from circle to triangle), we perform three types of analysis:

1. Saliency maps (heatmaps) of the predictor extracted by the XAI methods. These maps highlight the region of interest in the image for a machine learning model, as inferred by the given explainer.
2. Relational plots that visualize the correlation among the observed properties:
 - **Semantic variations** measures the degree of semantic variation between the varied images and the reference image.
 - **Saliency distances** denotes the mean squared deviation distances between the saliency maps of varied images and that of the reference image.
3. Statistical correlations between the changes in the input and the changes in distances between the heatmaps. We report Pearson correlation, Spearman’s rank correlation, and Kendall rank correlation (Kendall’s τ) to quantify the degree of explainer continuity.

The analysis of the first transformation (Rotation) can be seen in Figure 5. We can observe that GradCAM focuses on the edges of the triangle and shows a perfect explanation for the triangle class. When looking at the Saliency Distances for GradCAM in Figure 5b, GradCAM shows an oscillating pattern that matches the fact that after 60 degrees of rotation, the original image is obtained. Also, RISE shows the expected pattern for the rotation case with the exception

of a few outliers, although its explanations are less clear. The statistical correlations given in Table 5c match with these observations, note that for these statistics we only look at the first 30 degrees of change, as for those variations the saliency distances should be monotonically increasing. Lime fails to provide any differences in explanations and can therefore not be calculated. Note that with different hyper-parameters LIME could possibly be improved but that is outside the scope of this work.

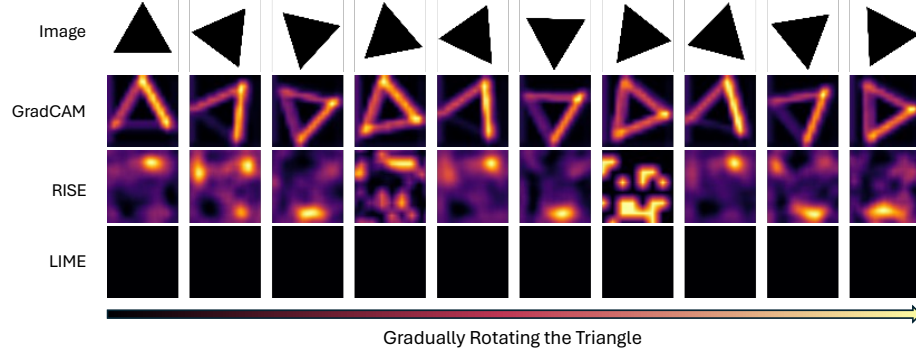
The analysis of the contrast transformation can be viewed in Figure 6. Visually, the explanations of GradCAM seem again to be superior, LIME in this case suffers from its binary nature in providing the explanations. Also, the relation between saliency distances and semantic variations in Figure 6b and the corresponding correlation metrics in Figure 6c confirms these observations. In the relation between distances and variations, GradCAM and RISE show the most monotonic pattern (GradCAM seems to be perfectly monotonically increasing), with Kendall’s Tau and Spearman giving highest correlation to GradCAM and Pearson correlation is the highest for RISE.

The analysis of the circle-to-triangle transformation can be viewed in Figure 7. Again GradCAM seems to be superior in terms of visualized explanations, however also RISE and LIME show meaningful and logical explanations in this case. In terms of the relation between the saliency distance and semantic variation, GradCAM suffers from the first few explanations being empty and a slight drop in saliency distance towards the end of the transformation, resulting in overall lower correlation measures than RISE for this case.

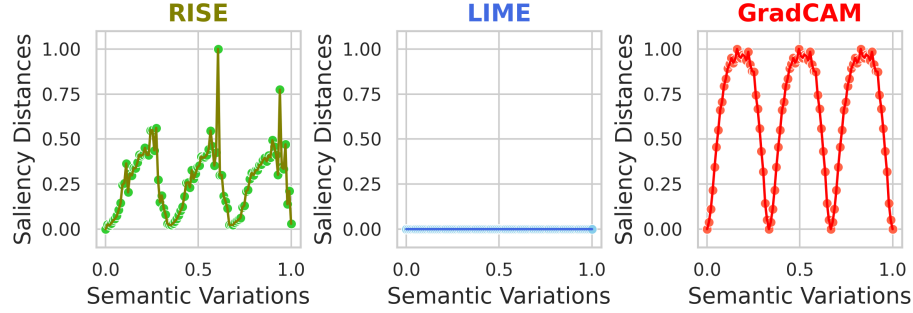
6.2 Synthesis facial dataset

In this section, we discuss the semantic continuity of the four evaluated XAI methods, case by case regarding different relationships between the semantic and the ResNet predictor. For each case, we present three types of analysis:

1. Saliency maps (heatmaps) of the predictor extracted by the XAI methods. These maps highlight the region of interest in the image for a machine learning model, as inferred by the given explainer.
2. Relational plots that visualize the correlation among the observed properties:
 - **Semantic variations** measures the degree of semantic variation between the varied images and the reference image.
 - **Model confidence** represents the probability of the given image to be of the class *with glasses*.
 - **Saliency distances** denotes the first Wasserstein distances between the saliency maps of varied images and that of the reference image.
 - **Confidence changes** quantifies the differences in model confidence between the varied to-be-measured images and the reference image.
3. Statistical correlations between the changes in model confidence and the changes in distances between the heatmaps. We report Pearson correlation and Kendall rank correlation (Kendall’s τ) to quantify the degree of explainer continuity as introduced in 4. Apart from the first Wasserstein distance, we



(a) The explanations from explainers regarding semantic variations. Darker areas suggest a higher impact on the model prediction.

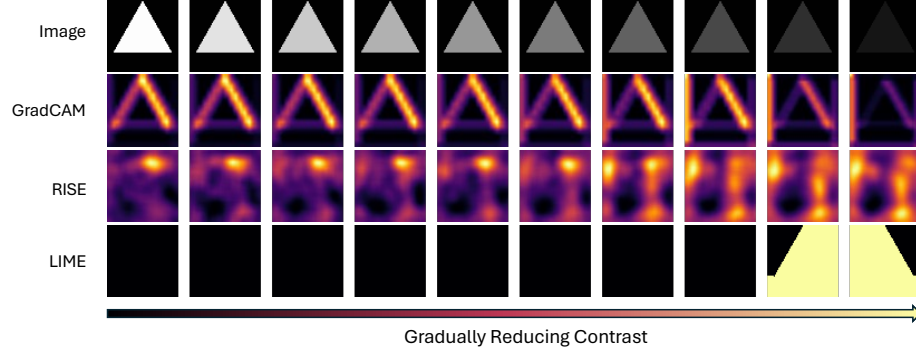


(b) The plots that portray the relation among semantic variation, and saliency distances. All variables are normalized to $[0, 1]$ for better visualization.

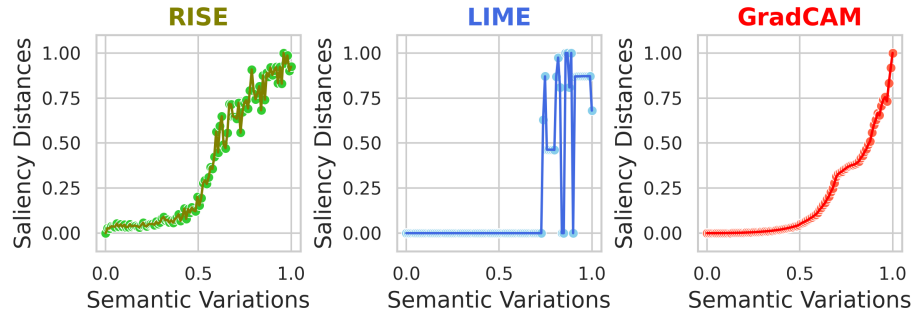
Correlation	Metric	RISE	LIME	GradCAM
Kendall	Wasserstein	0.383	-	0.733
	MSD	0.833	-	0.967
Pearson	Wasserstein	-	-	0.888
	MSD	0.935	-	0.958
Spearman	Wasserstein	-	-	0.865
	MSD	0.932	-	0.991

(c) Statistical correlations between the saliency distances and changes in the input for the first 30 degrees of change. The MSD stands for mean squared deviation, while the Wasserstein is the first Wasserstein distance. The highest correlation coefficient per metric per distance is colored in blue. The dash symbol, -, indicates a $p \geq 0.05$ where it is not evident enough to reject H_0 , i.e., the saliency distances and input changes are likely uncorrelated.

Fig. 5: **Rotation** transformation.



(a) The explanations from explainers regarding semantic variations. Darker areas suggest a higher impact on the model prediction.

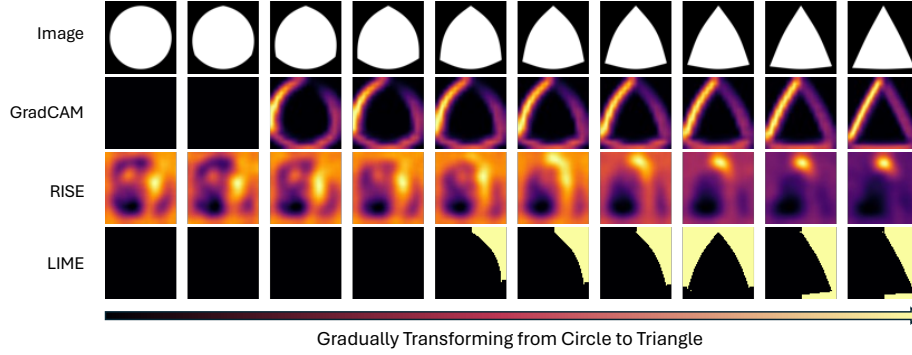


(b) The plots that portray the relation among semantic variation, and saliency distances. All variables are normalized to $[0, 1]$ for better visualization.

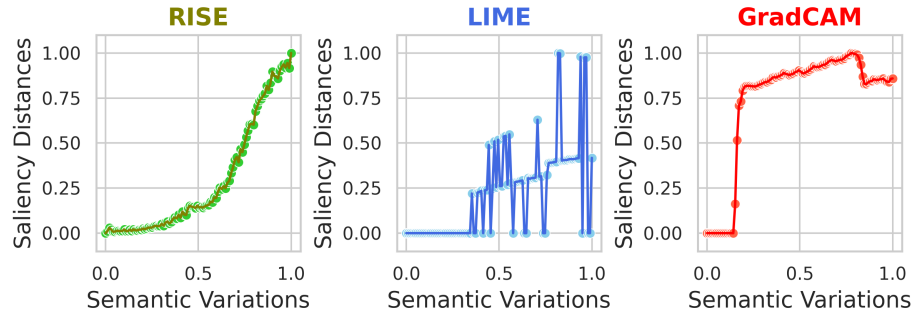
Correlation	Metric	RISE	LIME	GradCAM
Kendall	Wasserstein	0.788	0.580	0.926
	MSD	0.887	0.580	0.999
Pearson	Wasserstein	0.938	0.709	0.891
	MSD	0.941	0.709	0.879
Spearman	Wasserstein	0.939	0.717	0.979
	MSD	0.981	0.717	1.000

(c) Statistical correlations between the saliency distances and changes in the input. The MSD stands for mean squared deviation, while the Wasserstein is the first Wasserstein distance. The highest correlation coefficient per metric per distance is colored in **blue**. The dash symbol, -, indicates a $p \geq 0.05$ where it is not evident enough to reject H_0 , i.e., the saliency distances and input changes are likely uncorrelated.

Fig. 6: **Contrast** transformation.



(a) The explanations from explainers regarding semantic variations. Darker areas suggest a higher impact on the model prediction.



(b) The plots that portray the relation among semantic variation, and saliency distances. All variables are normalized to $[0, 1]$ for better visualization.

Correlation	Metric	RISE	LIME	GradCAM
Kendall	Wasserstein	0.784	0.633	0.523
	MSD	0.947	0.633	0.586
Pearson	Wasserstein	0.527	0.667	0.644
	MSD	0.916	0.667	0.671
Spearman	Wasserstein	0.909	0.719	0.541
	MSD	0.947	0.719	0.646

(c) Statistical correlations between the saliency distances and changes in the input. The MSD stands for mean squared deviation, while the Wasserstein is the first Wasserstein distance. The highest correlation coefficient per metric per distance is colored in blue. The dash symbol, -, indicates a $p \geq 0.05$ where it is not evident enough to reject H_0 , i.e., the saliency distances and input changes are likely uncorrelated.

Fig. 7: Circle to Triangle transformation.

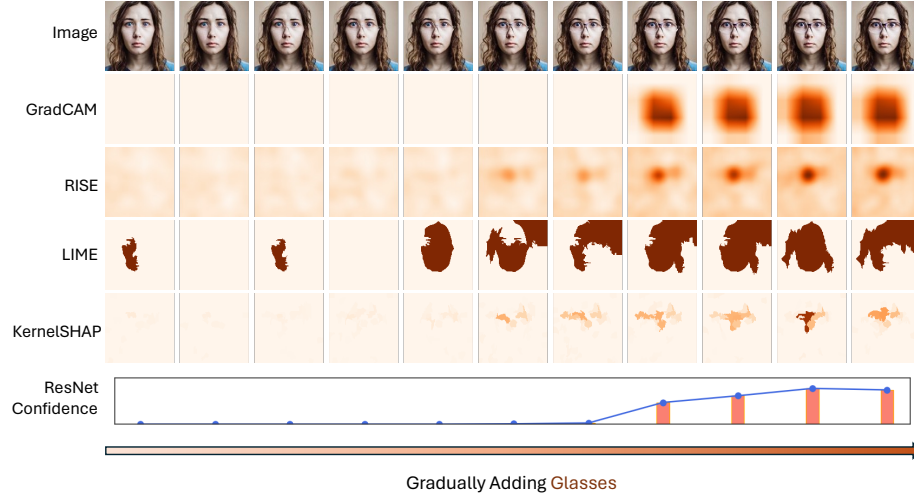
additionally report the correlation coefficients on saliency distances quantified by mean squared deviation between explanations.

We discuss our results regarding the four disjoint model’s predictive behaviour, commonly referred to as the confusion matrix. For convenience, interchangeably, we use **G** to denote GradCAM, **R** for RISE, **L** for LIME, and **K** for KernelSHAP.

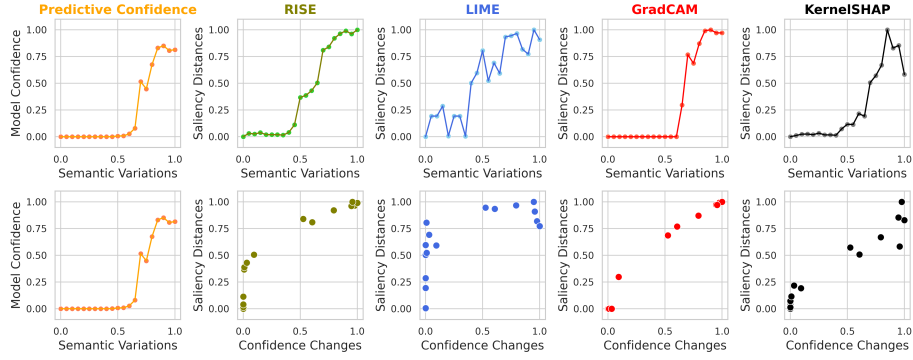
True positive The first case is a true positive as shown in Figure 8. The ResNet model correctly identifies the emergence of glasses of images as they are semantically varied from *no glasses* to *with glasses*. In Figure 8a, we display the saliency maps or the heatmaps produced by four explainers. Speaking intuitively based on the saliency maps, the G, R, and K correctly reflect the changes in model confidence regarding semantic variations as their (particularly R and K) highlight areas become darker and more concentrated on the locations of glasses. The qualitative relational plots in Figure 8b support these observations as G, R, and K possess stably coherent trends with the model’s predictive confidence, whereas the plots of LIME have strong stochasticity and do not display relatively monotonicity regarding the confidence changes. Figure 8c depicts the statistical correlations between the saliency distances and the changes in model confidence. With a significance level of 0.05, i.e., $p < 0.05$, we can find both linear and monotonical correlations between the saliency distances of all explainers and the changes in predictor’s confidence where GradCAM and RISE are believed to be more semantically continuous regarding the sizes of coefficients.

False positive Figure 9a illustrates a false positive scenario, wherein the model erroneously predicts the presence of glasses where the lenses are missing. All four explainers offer logical rationales: starting from the third column to the left in Figure 9a, the regions of interest are dense around the brow ridge and nasal bone, suggesting the model heavily weighs the presence of a glasses frame. The saliency maps contradict the trends of Wasserstein distance metrics. In Figure 9b, as the model’s confidence converges, the distance measurements from all explainers, except those from GradCAM, become stochastic and incoherent, whereas the saliency maps keep their consistency. Furthermore, empirical analysis through relational plots reveals that only GradCAM exhibits certain conformity with the predictor, while the KernelSHAP and RISE explainers behave similarly. The empirical findings are further substantiated by statistical correlation coefficients in 9c, where the discrepancies in GradCAM’s explanations demonstrate a stronger correlation with changes in model confidence. In contrast, it is unlikely that LIME is monotonic with the predictor judging by the correlation coefficients.

False negative In Figure 10, we present the analysis of false negatives. The model disbelieves the presence of glasses where they exist. Judging by the saliency maps shown in Figure 10a, RISE and KernelSHAP both exhibit a trend of the ResNet’s increasing focus on the right eye. LIME starts to produce a similar inference with KernelSHAP, i.e., highlighting hairs, and it later consistently inferred that the



(a) The explanations from explainers and the model confidence regarding semantic variations. Darker areas suggest a higher impact on the model prediction.

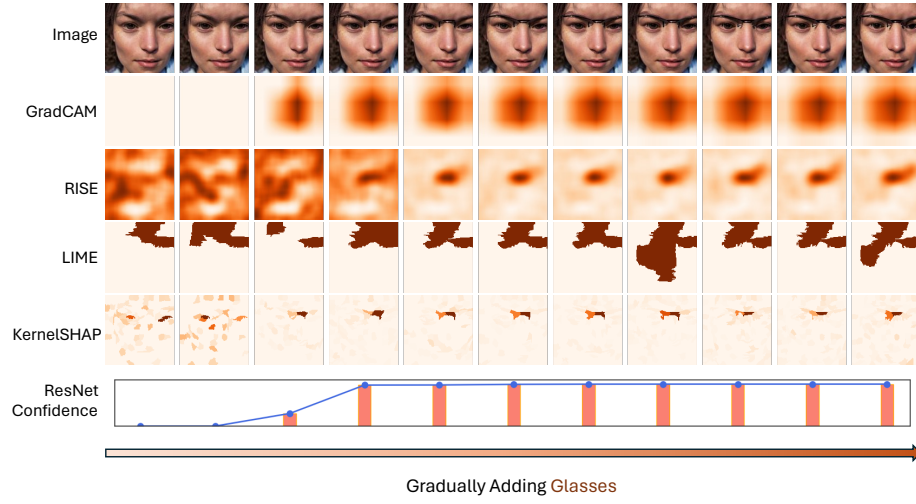


(b) The relation among semantic variation, model confidence, and saliency distances is visualized here. All variables are normalized to $[0, 1]$ for better visualization.

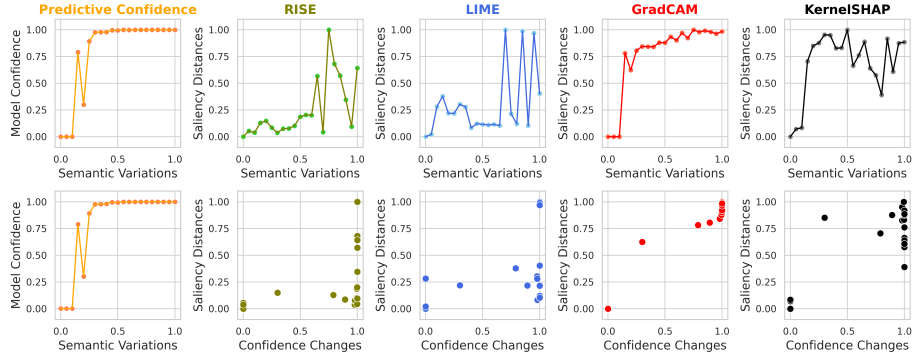
Correlation Metric	Distance	RISE	LIME	GradCAM	KernelSHAP
Kendall	Wasserstein	0.768	0.599	0.795	0.716
	MSD	0.863	0.599	0.795	0.758
Pearson	Wasserstein	0.930	0.745	0.989	0.716
	MSD	0.983	0.750	0.994	0.758
Spearman	Wasserstein	0.913	0.829	0.884	0.893
	MSD	0.965	0.820	0.884	0.908

(c) Statistical correlations between the saliency distances and changes in model confidence. The MSD stands for mean squared deviation, while the Wasserstein is the first Wasserstein distance. The highest correlation coefficient per metric per distance is colored in blue. We choose a threshold $p < 0.05$ to reject H_0 : the saliency distances and changes in model confidence are uncorrelated, and report the statistics.

Fig. 8: **True positive** example of no-glasses to glasses.



(a) The explanations from explainers and the model confidence regarding semantic variations. Darker areas suggest a higher impact on the model prediction.



(b) The plots portray the relation among semantic variation, model confidence, and saliency distances. All variables are normalized to $[0, 1]$ for better visualization.

Correlation	Metric	RISE	LIME	GradCAM	KernelSHAP
Kendall	Wasserstein	0.600	-	0.923	-
	MSD	0.779	-	0.923	-
Pearson	Wasserstein	-	-	0.957	0.693
	MSD	-	-	0.964	0.538
Spearman	Wasserstein	0.777	-	0.983	-
	MSD	0.923	-	0.983	-

(c) Statistical correlations between the saliency distances and changes in model confidence. The MSD stands for mean squared deviation, while the Wasserstein is the first Wasserstein distance. The highest correlation coefficient per metric per distance is colored in blue. The dash symbol, -, indicates a $p \geq 0.05$ where it is not evident enough to reject H_0 , i.e., the saliency distances and confidence changes are unlikely correlated.

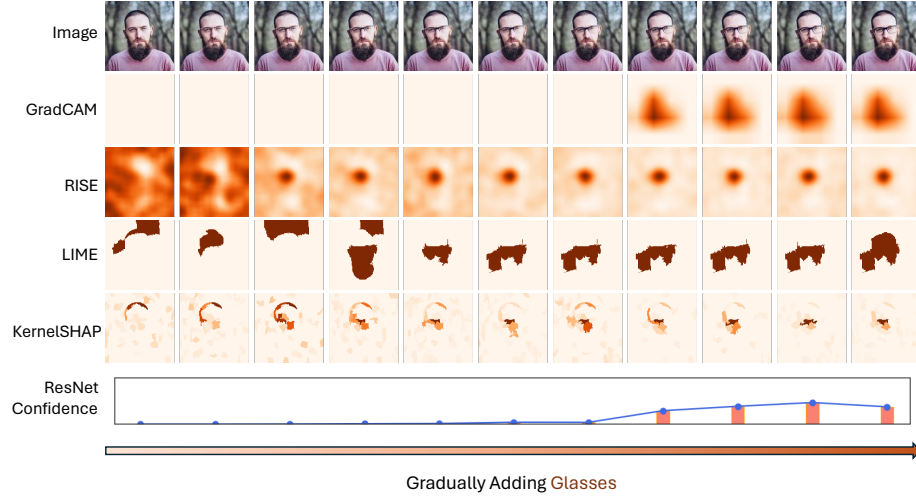
Fig. 9: **False positive** example of no-glasses to glasses.

ResNet focuses on both eyes. GradCAM’s inference says the predictor is more interested in the left cheek, which reasonably explains the cause of the predictor’s underperformance. The tendencies observed in RISE and KernelSHAP are also confirmed through relational plots. Empirically, we find out that GradCAM, KernelSHAP, and RISE each display a certain degree of monotonicity regarding the model confidence, whereas LIME is indifferent. Statistical analysis in Table 10c supports our empirical findings. It is hard to precisely rank the continuity of RISE, GradCAM, and KernelSHAP based on these tabular results, however, it is clear that LIME is the explainer with the least explainer continuity.

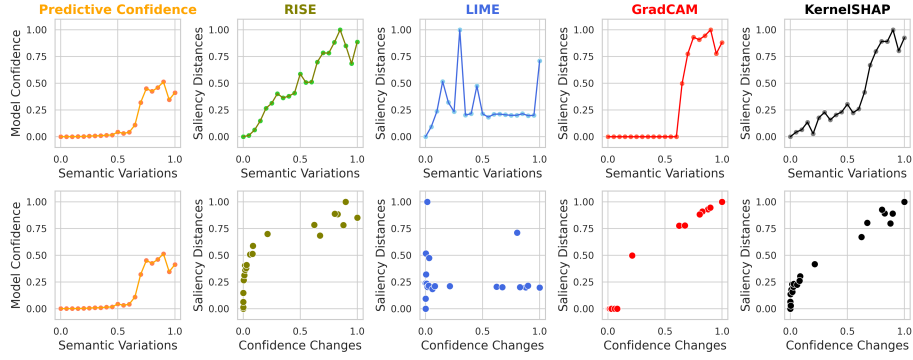
True negative This scenario in Figure 11 mirrors that depicted in Figure 11, but with a notable difference: ResNet avoids misclassifying images of eyeglasses without lenses (a **true negative**). Analysis of the heatmaps in Figure 11a reveals divergent explanatory behaviours: the heatmaps produced by GradCAM primarily shift between two patterns; RISE’s interpretations appear randomly distributed; LIME’s explanations concentrate on the upper right segments of the images, albeit with some fluctuation; KernelSHAP consistently emphasizes both eyebrows. Empirical observations from relational plots in Figure 11b and statistical results in Table 11c indicate that GradCAM and KernelSHAP maintain certain explainer continuity regarding predictors, in contrast to the discontinuity exhibited partially by LIME and particularly by RISE despite low yet stable model confidence.

Summarizing our analysis across four case studies, visual inspection of saliency maps shows that KernelSHAP delivers the most semantically continuous and informative explanations. RISE and GradCAM follow, ranked second and third, respectively, while LIME is the least informative, with discontinuity between closely adjacent semantics. Regarding metric studies through relational plots and statistical correlations, GradCAM undoubtedly is the most semantically continuous explainer, with KernelSHAP, RISE, and LIME following in descending order.

Besides summarizing findings on an explainer level, we discuss the conformity between qualitative, and our proposed quantitative analysis. Among three of the four studied cases, in Figure 8, Figure 9, and Figure 10, analytical observations on statistical correlation (linearity and monotonicity) between the saliency distances and the changes in model confidence generally match and support our empirical findings on explanations and relational plots.



(a) The explanations from explainers and the model confidence regarding semantic variations. Darker areas suggest a higher impact on the model prediction.

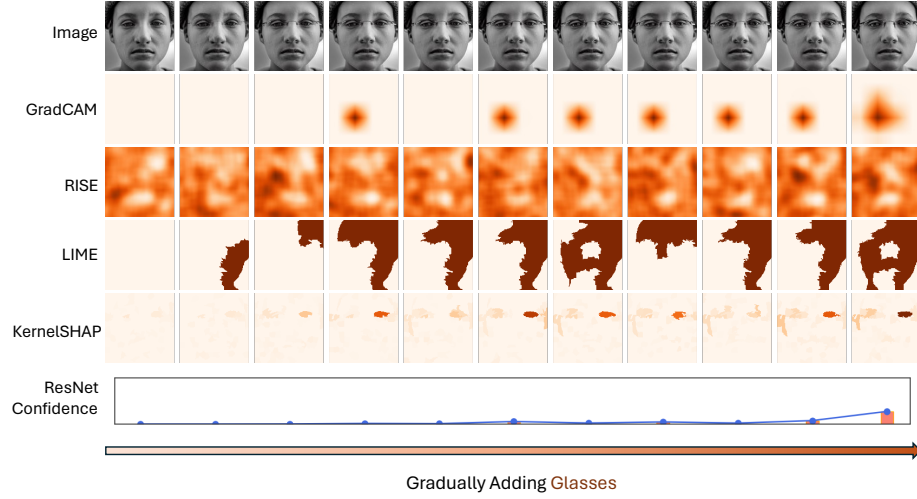


(b) The plots portray the relation among semantic variation, model confidence, and saliency distances. All variables are normalized to $[0, 1]$ for better visualization.

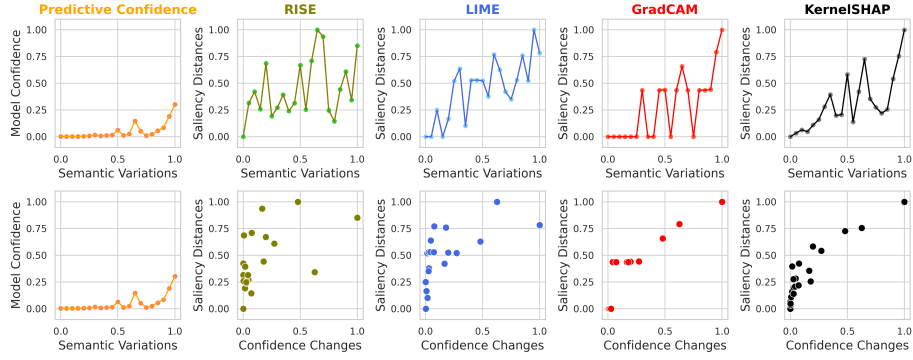
Correlation	Metric	RISE	LIME	GradCAM	KernelSHAP
Kendall	Wasserstein	0.884	-	0.808	0.886
	MSD	0.863	0.421	0.795	0.884
Pearson	Wasserstein	0.866	-	0.984	0.981
	MSD	0.927	0.52	0.983	0.972
Spearman	Wasserstein	0.967	-	0.886	0.958
	MSD	0.961	0.612	0.884	0.974

(c) Statistical correlations between the saliency distances and changes in model confidence. The MSD stands for mean squared deviation, while the Wasserstein is the first Wasserstein distance. The highest correlation coefficient per metric per distance is colored in **blue**. The dash symbol, -, indicates a $p \geq 0.05$ where it is not evident enough to reject H_0 , i.e., the saliency distances and confidence changes are likely uncorrelated.

Fig. 10: **False negative** example of no-glasses to glasses.



(a) The explanations from explainers and the model confidence regarding semantic variations. Darker areas suggest a higher impact on the model prediction.



(b) The plots that portray the relation among semantic variation, model confidence, and saliency distances. All variables are normalized to $[0, 1]$ for better visualization.

Correlation	Metric	RISE	LIME	GradCAM	KernelSHAP
Kendall	Wasserstein	-	0.617	0.807	0.758
	MSD	-	0.617	0.847	0.695
Pearson	Wasserstein	0.897	0.616	0.851	0.907
	MSD	0.616	0.616	0.832	0.957
Spearman	Wasserstein	0.48	0.801	0.924	0.887
	MSD	-	0.801	0.939	0.842

(c) Statistical correlations between the saliency distances and changes in model confidence. The MSD stands for mean squared deviation, while the Wasserstein is the first Wasserstein distance. The highest correlation coefficient per metric per distance is colored in blue. The dash symbol, -, indicates a $p \geq 0.05$ where it is not evident enough to reject H_0 , i.e., the saliency distances and confidence changes are likely uncorrelated.

Fig. 11: **True negative** example of no-glasses to glasses.

7 Conclusions and Outlook

In this paper, we presented a novel methodology for evaluating semantic continuity for Explainable AI (XAI) methods and subsequently the predictive models. Our focus on semantic continuity emphasizes the importance of consistent explanations for similar inputs. We characterize an explainer as semantically continuous if similar inputs, lead to similar model predictions, having similar explanations. We explored semantic continuity for image classification tasks, assessing how sequential input changes impact the DL model explanations. We explored popular explainers, including LIME, RISE, GradCAM and KernelSHAP.

We performed an in-depth instance-based analysis for a realistic and complex image binary classification task and different XAI methods. We found that regarding the relational plots and statistical correlations, GradCAM shows to be the most semantically continuous explainer, with KernelSHAP following as a good second. Visual inspection results of saliency maps are mostly in agreement with the proposed qualitative and quantitative semantic continuity measures.

The investigation of semantic continuity extends our understanding of the interpretability of DL models and the capacities of different XAI methods, introducing a crucial dimension to the evaluation of XAI methods.

Numerous promising avenues exist for future research in the intersection of semantic continuity and XAI. First, the proposed metric can be further extended to support different types of deep learning tasks beyond image classification and also extend to other domains, such as text or speech. Additionally, exploring the impact of semantic continuity on user trust and acceptance of DL models and XAI methods can provide insights into the practical implications of our findings. To quantify the semantic continuity, different metrics could be explored such as Distance correlation [33]. In conclusion, we hope that our comprehension of semantic continuity and its nuanced implications not only enhances the evolution of Explainable AI methods but also supports the usage of deep learning across diverse domains.

Disclosure of Interests. The authors have no competing interests to declare that are relevant to the content of this article.

Acknowledgments

We would like to thank the Lorentz Center for organizing the Workshop; ICT with Industry, which led to the collaboration and this work. This publication is part of the project XAIPre (with project number 19455) of the research program Smart Industry 2020 which is (partly) financed by the Dutch Research Council (NWO). Funding for Osman Mutlu in this research has been provided by the European Union’s Horizon Europe research and innovation programme EFRA [grant number 101093026].

References

1. Brack, M., Friedrich, F., Hintersdorf, D., Struppek, L., Schramowski, P., Kersting, K.: SEGA: Instructing text-to-image models using semantic guidance. In: Thirty-seventh Conference on Neural Information Processing Systems (2023), <https://openreview.net/forum?id=KIPAIy329j>
2. Cugny, R., Aligon, J., Chevalier, M., Roman Jimenez, G., Teste, O.: Autoxai: A framework to automatically select the most adapted xai solution. In: Proceedings of the 31st ACM International Conference on Information & Knowledge Management. pp. 315–324 (2022)
3. Galli, A., Marrone, S., Moscato, V., Sansone, C.: Reliability of explainable artificial intelligence in adversarial perturbation scenarios. In: Del Bimbo, A., Cucchiara, R., Sclaroff, S., Farinella, G.M., Mei, T., Bertini, M., Escalante, H.J., Vezzani, R. (eds.) Pattern Recognition. ICPR International Workshops and Challenges. pp. 243–256. Springer International Publishing, Cham (2021)
4. He, K., Zhang, X., Ren, S., Sun, J.: Deep residual learning for image recognition (2015)
5. Hedström, A.: Explainable Artificial Intelligence : How to Evaluate Explanations of Deep Neural Network Predictions using the Continuity Test. Master’s thesis, KTH, School of Electrical Engineering and Computer Science (EECS) (2020)
6. Hedström, A., Weber, L., Krakowczyk, D., Bareeva, D., Motzkus, F., Samek, W., Lapuschkin, S., Höhne, M.M.M.: Quantus: An explainable ai toolkit for responsible evaluation of neural network explanations and beyond. *Journal of Machine Learning Research* **24**(34), 1–11 (2023), <http://jmlr.org/papers/v24/22-0142.html>
7. Huang, W., Zhao, X., Jin, G., Huang, X.: Safari: Versatile and efficient evaluations for robustness of interpretability. In: Proceedings of the IEEE/CVF International Conference on Computer Vision. pp. 1988–1998 (2023)
8. Kamath, S., Mittal, S., Deshpande, A., Balasubramanian, V.N.: Rethinking robustness of model attributions (2023)
9. Kendall, M.G.: A new measure of rank correlation. *Biometrika* **30**(1/2), 81–93 (1938)
10. Kingma, D.P., Ba, J.: Adam: A method for stochastic optimization (2017)
11. Kokhlikyan, N., Miglani, V., Martin, M., Wang, E., Alsallakh, B., Reynolds, J., Melnikov, A., Kliushkina, N., Araya, C., Yan, S., et al.: Captum: A unified and generic model interpretability library for pytorch. arXiv preprint arXiv:2009.07896 (2020)
12. Le, P.Q., Nauta, M., Nguyen, V.B., Pathak, S., Schlötterer, J., Seifert, C.: Benchmarking explainable ai - a survey on available toolkits and open challenges. In: Elkind, E. (ed.) Proceedings of the Thirty-Second International Joint Conference on Artificial Intelligence, IJCAI-23. pp. 6665–6673. International Joint Conferences on Artificial Intelligence Organization (8 2023). <https://doi.org/10.24963/ijcai.2023/747>, <https://doi.org/10.24963/ijcai.2023/747>, survey Track
13. Liu, Y., Khandagale, S., White, C., Neiswanger, W.: Synthetic benchmarks for scientific research in explainable machine learning. In: Advances in Neural Information Processing Systems Datasets Track (2021)
14. Liu, Y., Meijer, C., Oostrum, L.: Onnx model trained on the simple geometric dataset (Jan 2022). <https://doi.org/10.5281/zenodo.5907059>, <https://doi.org/10.5281/zenodo.5907059>

15. Lopes, P., Silva, E., Braga, C., Oliveira, T., Rosado, L.: Xai systems evaluation: A review of human and computer-centred methods. *Applied Sciences* **12**(19), 9423 (2022)
16. Lundberg, S.M., Lee, S.I.: A unified approach to interpreting model predictions. *Advances in neural information processing systems* **30** (2017)
17. Nauta, M., Seifert, C.: The co-12 recipe for evaluating interpretable part-prototype image classifiers. In: *World Conference on Explainable Artificial Intelligence*. pp. 397–420. Springer (2023)
18. Nauta, M., Trienes, J., Pathak, S., Nguyen, E., Peters, M., Schmitt, Y., Schlötterer, J., van Keulen, M., Seifert, C.: From anecdotal evidence to quantitative evaluation methods: A systematic review on evaluating explainable ai. *ACM Computing Surveys* **55**(13s), 1–42 (2023)
19. Oostrum, L., Liu, Y., Meijer, C., Rangelova, E., Bos, P.: Simple geometric shapes (Jul 2021). <https://doi.org/10.5281/zenodo.5012825>, <https://doi.org/10.5281/zenodo.5012825>
20. Park, C., Yang, S., Na, I., Chung, S., Shin, S., Kwon, B.C., Park, D., Choo, J.: VATUN: Visual Analytics for Testing and Understanding Convolutional Neural Networks. In: Agus, M., Garth, C., Kerren, A. (eds.) *EuroVis 2021 - Short Papers*. The Eurographics Association (2021). <https://doi.org/10.2312/evs.20211047>
21. Pearson, K.: Notes on regression and inheritance in the case of two parents proceedings of the royal society of london, 58, 240-242. K Pearson (1895)
22. Petsiuk, V., Das, A., Saenko, K.: Rise: Randomized input sampling for explanation of black-box models. *arXiv preprint arXiv:1806.07421* (2018)
23. Rangelova, E., Bos, P., Liu, Y., Meijer, C., Oostrum, L., Crocioni, G., Jansen, A., Ootes, L., Chandramouli, P., Smeets, S., van der Spek, W.: dianna. <https://doi.org/10.5281/zenodo.5801485>, <https://github.com/dianna-ai/dianna>
24. Rangelova, E., Meijer, C., Oostrum, L., Liu, Y., Bos, P., Crocioni, G., Lanouvelle, M., Guevara, B.C., Bakhshi, R., Podareanu, D.: Dianna: Deep insight and neural network analysis. *Journal of Open Source Software* **7**(80), 4493 (2022). <https://doi.org/10.21105/joss.04493>, <https://doi.org/10.21105/joss.04493>
25. Ribeiro, M.T., Singh, S., Guestrin, C.: " why should i trust you?" explaining the predictions of any classifier. In: *Proceedings of the 22nd ACM SIGKDD international conference on knowledge discovery and data mining*. pp. 1135–1144 (2016)
26. Rombach, R., Blattmann, A., Lorenz, D., Esser, P., Ommer, B.: High-resolution image synthesis with latent diffusion models. In: *Proceedings of the IEEE/CVF Conference on Computer Vision and Pattern Recognition (CVPR)*. pp. 10684–10695 (June 2022)
27. Samek, W.: Explainable deep learning: concepts, methods, and new developments. In: *Explainable Deep Learning AI*, pp. 7–33. Elsevier (2023)
28. Selvaraju, R.R., Cogswell, M., Das, A., Vedantam, R., Parikh, D., Batra, D.: Gradcam: Visual explanations from deep networks via gradient-based localization. In: *Proceedings of the IEEE international conference on computer vision*. pp. 618–626 (2017)
29. Shen, Y., Yang, C., Tang, X., Zhou, B.: Interfacegan: Interpreting the disentangled face representation learned by gans. *TPAMI* (2020)
30. Sietzen, S., Lechner, M., Borowski, J., Hasani, R., Waldner, M.: Interactive analysis of cnn robustness. *Computer Graphics Forum* **40**(7), 253–264 (2021). <https://doi.org/https://doi.org/10.1111/cgf.14418>, <https://onlinelibrary.wiley.com/doi/abs/10.1111/cgf.14418>

31. Spearman, C.: The proof and measurement of association between two things. *The American journal of psychology* **100**(3/4), 441–471 (1987)
32. Stein, B.V., Raponi, E., Sadeghi, Z., Bouman, N., Van Ham, R.C.H.J., Bäck, T.: A comparison of global sensitivity analysis methods for explainable ai with an application in genomic prediction. *IEEE Access* **10**, 103364–103381 (2022). <https://doi.org/10.1109/ACCESS.2022.3210175>
33. Székely, G.J., Rizzo, M.L., Bakirov, N.K.: Measuring and testing dependence by correlation of distances (2007)
34. Wu, S., Sang, J., Zhao, X., Chen, L.: An experimental study of semantic continuity for deep learning models (2020)
35. Yang, M., Kim, B.: Benchmarking Attribution Methods with Relative Feature Importance. *CoRR* **abs/1907.09701** (2019)
36. Yang, W., Le, H., Savarese, S., Hoi, S.: Omnixai: A library for explainable ai (2022). <https://doi.org/10.48550/ARXIV.2206.01612>, <https://arxiv.org/abs/2206.01612>